

NATURE OF THE EXTREME ULTRALUMINOUS X-RAY SOURCES

GRZEGORZ WIKTOROWICZ¹, MAŁGORZATA SOBOLEWSKA², ALEKSANDER SĄDOWSKI³ KRZYSZTOF BELCZYŃSKI^{1, 4}

¹ Astronomical Observatory, Warsaw University, Al. Ujazdowskie 4, 00-478 Warsaw, Poland (gwiktoro@astrouw.edu.pl)

² Nicolaus Copernicus Astronomical Center, Bartycka 18, 00-716 Warsaw, Poland

³ MIT Kavli Institute for Astrophysics and Space Research 77 Massachusetts Ave, Cambridge, MA 02139, USA

⁴ Warsaw Virgo Group

Draft version September 24, 2018

ABSTRACT

In this proof-of-concept study we demonstrate how a binary system can *easily* form an extreme ULX source with the X-ray luminosity of $L_x \gtrsim 10^{42} \text{ erg s}^{-1}$. Formation efficiencies and lifetimes of such objects are high enough to potentially explain *all* observed extreme ULXs. These systems are not only limited to binaries with stellar-origin black hole accretors. Noteworthy, we have also identified such objects with neutron stars. Typically, a $10 M_\odot$ black hole is fed by a massive ($\sim 10 M_\odot$) Hertzsprung gap donor with Roche lobe overflow rate of $\sim 10^{-3} M_\odot \text{ yr}^{-1}$ ($\approx 2600 \dot{M}_{\text{Edd}}$). For neutron star systems the typical donors are evolved low-mass ($\sim 2 M_\odot$) helium stars with Roche lobe overflow rate of $\sim 10^{-2} M_\odot \text{ yr}^{-1}$. We base our study *purely* on the available Roche lobe overflow rate in a binary system and show that if only even a small fraction ($\gtrsim 10^{-3}$) of the overflow reaches the BH, the source will be super-Eddington. Our study does not prove that any particular extreme ULX (e.g., HLX-1) is a regular binary system with a rather low-mass compact object (a stellar-origin black hole or a neutron star). However, it demonstrates that *any* ULX, including the most luminous ones, may potentially be a short-lived phase in the life of a binary star.

Subject headings: stars: black holes, neutron stars, X-ray binaries

1. INTRODUCTION

Our Universe is populated with black holes (BH) and neutron stars (NS) in various binary configurations. In our Galaxy, many such binaries show significant X-ray activity suggestive of a mass transfer and accretion onto the compact star. X-ray luminosities of Galactic X-ray binaries (XRBs) exceed $\sim 10^{39} \text{ erg s}^{-1}$ (approximately the Eddington limit for a $10 M_\odot$ BH) in only two systems (GRS 1915+105, SS 433; Fender & Belloni 2004; Fabrika et al. 2006).

However, a large population of extra-galactic point-like X-ray sources with luminosities in excess of $\sim 10^{39} \text{ erg s}^{-1}$ has been identified (e.g., Fabbiano et al. 1989; Liu 2011; Walton et al. 2011). These so-called Ultraluminous X-ray sources (ULX) are off-nuclear and therefore accretion onto a supermassive BH ($M > 10^5 M_\odot$) can be excluded as the source of their luminosity. Instead, the two most popular scenarios to explain their nature include binary systems hosting (*i*) a stellar mass BH accreting at a super-Eddington rate, or (*ii*) an intermediate mass BH (IMBH) and sub-Eddington accretion (Colbert & Mushotzky 1999). In the latter case, formation of BHs heavier than $\sim 100 M_\odot$ presents a problem for current models of stellar evolution. Although it has been suggested that such IMBHs may be formed in dense globular clusters (Miller & Hamilton 2002) or even as a result of stellar evolution of very massive stars ($\sim 200 - 300 M_\odot$; Crowther et al. 2010; Yusof et al. 2013).

The super-Eddington BH accretion invoked in the stellar origin scenario remains still a relatively poorly understood regime. However, several theoretical mechanisms able to breach the Eddington limit have been proposed, e.g., beaming and/or hyper-accretion allowed by non-uniform escape of photons from accretion flow ("photonic

bubbles") (King et al. 2001; Begelman et al. 2006; Poutanen et al. 2007; King 2008), photon trapping in slim disk accretion (Ohsuga 2007a; Abramowicz & Straub 2008; Narayan et al. 2012; Sądowski et al. 2015), as well as a contribution of rotation powered pulsars and pulsar wind nebulae to the ULX population (Medvedev & Poutanen 2013).

Robust observational constraints on the mass of the accretor in some ULXs (e.g., Motch et al. 2014) indicate that indeed super-Eddington accretion is realized in nature. Additionally some sources transit relatively fast between the super- and sub-Eddington regimes on timescales as short as a few days to a week (e.g., Walton et al. 2013; Bachetti et al. 2013). Moreover, Bachetti et al. (2014) have demonstrated that the super-Eddington accretion is also possible in XRBs hosting a NS. Nevertheless, it has been speculated that the brightest ULXs, with luminosities $> 10^{41} \text{ erg s}^{-1}$ (Hyperluminous X-ray sources; HLXs) may be candidate IMBHs (e.g., Sutton et al. 2012) or even background AGNs (Sutton et al. 2015). At the moment HLX-1 with $L_x = 1.1 \times 10^{42} \text{ erg s}^{-1}$ (Farrell et al. 2011) is the brightest known ULX (for a discussion of the brightest ULXs see Servillat et al. 2011). Recently, compelling evidence was presented in support of a $\sim 400 M_\odot$ BH in an ULX located in M82 (Pasham et al. 2014).

We approach the ULX issue from the standpoint of one particular evolutionary model for binary evolution. We consider only the far end of the ULX luminosity space, $L_x \gtrsim 10^{42} \text{ erg s}^{-1}$, and we refer to the sources potentially able to reach these luminosities as extreme ULXs (EULXs). We explore the possibility that EULXs are binary systems that accrete at rates exceeding classical Eddington limit.

2. MODEL

We employ the binary population synthesis code, *StarTrack* (Belczynski et al. 2008a), with updates as discussed in Dominik et al. (2014). We use the BOINC platform¹ for volunteer computing in our program ‘‘Universe@home’’ (<http://universeathome.pl>) to obtain a large number of X-ray binaries ($N = 10^9$ of massive binary systems were evolved by volunteers). The X-ray binary is defined as a system hosting a donor star transferring mass via Roche lobe overflow (RLOF) to a compact object companion (NS or BH). For any given system our evolutionary models provide the donor RLOF mass transfer rate (\dot{M}_{RLOF}). The accretion rate onto a compact object (\dot{M}_{acc}) is estimated in three different ways from the mass transfer rate (see below).

First, we have assumed that the fraction of RLOF mass transfer which is accreted is 1.0, i.e. the mass accretion rate $\dot{M}_{\text{acc}} = \dot{M}_{\text{RLOF}}$ even for very high RLOF mass transfer rates.

Secondly, we have considered a BH accretion case with $\dot{M}_{\text{acc}} < \dot{M}_{\text{RLOF}}$, where the mass accretion at the BH, \dot{M}_{acc} , is constrained following the results of Ohsuga (2007a) who performed global, axisymmetric simulations of super-critical disks with the αP viscosity. We use the parametrization of this model as a function of the input mass accretion rate, \dot{M}_{RLOF} , derived in Belczynski et al. (2008b). The remainder of the mass transferred through the RLOF is assumed to be ejected from the system. The accretion onto NSs is limited to classical Eddington limit in this model.

In the both cases the XRB X-ray luminosity is calculated as

$$L_x = \epsilon GM_{\text{acc}} \dot{M}_{\text{acc}} / R_{\text{acc}} \quad (1)$$

where the radius of the accretor, R_{acc} , is 10 km for a NS and 3 Schwarzschild radii for a BH, and ϵ gives a conversion efficiency of gravitational binding energy to radiation associated with accretion onto a NS (surface accretion $\epsilon = 1.0$) and onto a BH (disk accretion $\epsilon = 0.5$)². In the case in which we do not impose any upper limit on the accretion rate, and convert the donor RLOF rate directly into accretion rate we obtain the maximum potential X-ray of a given binary ($L_{x,\text{max}}$).

Finally, we have experimented with the constraints on the \dot{M}_{acc} and L_x following the recent results of Sądowski et al. (2015) who found a considerable amount of beaming in their simulations of super-Eddington accretion disks. The accretion rate at the BH horizon was found to be only a fraction of the RLOF rate,

$$\dot{M}_{\text{acc}} = \dot{M}_{\text{RLOF}} \frac{R_{\text{wind}}}{R_{\text{out}}}, \quad (2)$$

where R_{out} is the outer radius of the wind emitting region and $R_{\text{wind}} \approx 20R_g$ is the inner radius of the wind emitting region (Sądowski et al. 2014). It is hard to estimate the size of the wind emitting region, so we assumed a constant fraction $R_{\text{wind}}/R_{\text{out}} = 0.01$. The X-ray lumi-

nosity is then calculated from

$$L_x = 4 \times 10^{38} \times e^{-\frac{\theta}{0.2}} \frac{\dot{M}_{\text{acc}}}{\dot{M}_{\text{Edd}}} \frac{M_{\text{BH}}}{M_{\odot}} \text{erg s}^{-1}, \quad (3)$$

where θ is the viewing angle, $\dot{M}_{\text{Edd}} = 2.44 \times 10^{18} \frac{M}{M_{\odot}} \text{g s}^{-1}$ is the Eddington accretion rate. In our simulations we incorporated θ in the range 0 – 0.5 and for every system we calculated the probability of observing the source with X-ray luminosity above $10^{42} \text{erg s}^{-1}$. We note that the results of Ohsuga (2007a) can be put in the framework of this model by taking $R_{\text{out}} \approx 50R_g$, which is approximately the effective circularization radius (and the outer edge of the disk) of the gas injected into their simulation box. For NS accretors we assumed that the prescription is the same as for the BHs.

We search for evolutionary channels that allow for the formation of binaries with RLOF rates onto BH or NS from H-rich or He-rich donor at rates that exceed $L_{x,\text{max}} > 10^{42} \text{erg s}^{-1}$. Conservatively, we model only solar metallicity ($Z_{\odot} = 0.02$; Villante et al. 2014)) and we allow initial mass function (IMF) to extend only to $150 M_{\odot}$. Note that lower metallicity and higher mass stars may form massive ($\gtrsim 100 M_{\odot}$) black holes in binary systems (Belczynski et al. 2014).

3. RESULTS

Under the least restricting assumption (no limit on accretion rate) our EULX rate/number estimates are only upper limits. We find that 1 star per 43 billion could potentially be an EULX. If the accretors are limited to BHs only 1 star per 87 billions could be a potential EULX. This estimate employs a canonical IMF (Kroupa & Weidner 2003) and 50% binary fraction.

Figure 1 shows our upper limits for the number of EULXs with BH and NS accretors. Note that we obtain virtually as many potential EULXs with a NS as with a BH accretor. This estimate accounts for the specific lifetime of each binary in a potential EULX phase. We assumed that the typical density of Milky Way Equivalent galaxies (MWEG) in the local universe is $\rho_{\text{MWEG}} = 0.01 \text{Mpc}^{-3}$. Currently, the observations place the only confirmed EULX (HLX-1) at the distance of 95 Mpc (Wiersema et al. 2010, but see Lasota et al. (2015)). Our predicted upper limit on the number of EULXs at this distance is 90 and 93 binaries with BH and NS accretors, respectively. Both estimates significantly exceed the observed number of sources.

Table 1 introduces typical companion stars of our EULXs. Majority of the NS EULXs (92%) are found in binaries with Helium star donors: either a $\sim 1.2 M_{\odot}$ Helium Hertzsprung gap star (HeHg) or $\sim 1.8 M_{\odot}$ Helium Giant Branch (HeGB) star. The BH EULXs predominantly contain a hydrogen-rich stars that have just evolved beyond main sequence. Typically, these are $\sim 6 M_{\odot}$ Hertzsprung gap (HG) stars (92.4%). The mass distributions of these most common EULX companions are presented in Fig. 2. Table 2 contains typical evolutionary routes that lead to the formation of EULXs.

As a result of implementing the slim disk model of Ohsuga (2007a), the X-ray luminosities of our systems drop by a factor of at least 2.8. Nevertheless, in this framework it is still possible to significantly exceed the classical Eddington limit. The estimated number of the

¹ <http://boinc.berkeley.edu/>

² Equivalently, $L_{x,\text{max}} = \eta \dot{M}_{\text{acc}} c^2$, where η is the accretion efficiency, and in our case $\eta_{\text{BH}} = 1/12$, $\eta_{\text{NS}} \simeq 0.2$.

BH EULX systems decreases to 1 in 210 billion stars, and the number of BH EULXs within 100 Mpc is 37 (Fig. 1).

In the prescription of Sądowski et al. (2015) the upper limit on a number of expected EULX drops to 1 per 2×10^{15} stars. The expected upper limit on the number of EULX systems in the distance range of HLX-1 is 0.004. This is four orders of magnitude less than in the two other models we tested.

Had we imposed the classical Eddington limit on the mass accretion rate in our modeling, the number of EULXs would be zero for both types of accretors.

In all cases, the EULX luminosities are achieved during the thermal timescale RLOF. The RLOF mass transfer rate is calculated following Kalogera & Webbink (1996) as

$$\dot{M}_{\text{RLOF,th}} = \frac{M_{\text{don}}}{\tau_{\text{th}}} = \frac{1}{3} \times 10^{-7} \frac{R_{\text{don}} L_{\text{don}}}{M_{\text{don}}} M_{\odot} \text{ yr}^{-1} \quad (4)$$

where donor mass, radius and luminosity are expressed in solar units. For example an EULX with a BH can start with a $\sim 10 M_{\odot}$ Hertzsprung gap donor, that has $\sim 20 R_{\odot}$ radius and luminosity of $\sim 2 \times 10^4 L_{\odot}$. The donors in NS systems are evolved (post core He-burning) low-mass Helium stars that on the onset of RLOF have mass $\sim 2 M_{\odot}$, radius $\sim 30 R_{\odot}$ and luminosity $\sim 2 \times 10^4 L_{\odot}$. These parameters allow for the possibility of very high RLOF mass transfer rates ($\dot{M}_{\text{RLOF,th}} \sim 10^{-2} - 10^{-3} M_{\odot} \text{ yr}^{-1}$; corresponding to $L_{\text{x,max}} \gtrsim 10^{42} - 10^{43} \text{ erg s}^{-1}$) alas on a very short timescale ($\tau_{\text{th}} \sim 10^2 - 10^4 \text{ yr}$).

Typical evolutionary routes that lead to the formation of a potential BH and NS EULX when $\dot{M}_{\text{acc}} = \dot{M}_{\text{RLOF}}$ are detailed in Secs. 3.1–3.2. The corresponding time behavior of the mass accretion rate and maximum X-ray luminosity are shown in Figures 3 and 4.

3.1. Black hole EULX

A typical BH EULX system evolves along the evolutionary channel presented in Table 2. Its evolution begins with a $33 M_{\odot}$ primary and $11 M_{\odot}$ secondary on an orbit with separation $\sim 5500 R_{\odot}$ and eccentricity $e = 0.56$. In 5.5 Myr the primary starts crossing the Hertzsprung gap (HG). At that point the orbit has expanded to $5900 R_{\odot}$ due to wind mass loss from the primary (now $30 M_{\odot}$). After about 10,000 yr and significant radial expansion ($1300 R_{\odot}$), the primary begins core helium burning (CHeB). As the primary approaches its Roche lobe tidal interactions circularize the orbit. After some additional expansion (radius $1700 R_{\odot}$) and mass loss the primary ($18 M_{\odot}$) initiates a common envelope (CE) phase. Following the envelope ejection the orbit contracts to $40 R_{\odot}$ and the primary becomes a Wolf-Rayet (WR) star with the mass of $11 M_{\odot}$. After 6.2 Myr of evolution the primary undergoes a core collapse and forms a $7.2 M_{\odot}$ BH. At this time the orbit is rather compact ($a = 47 R_{\odot}$) and almost circular ($e = 0.04$).

After the next 13 Myr the secondary enters the HG with a mass of $11 M_{\odot}$ and radius $10 R_{\odot}$, and expands filling its Roche lobe ($R_{\text{lobe}} = 19 R_{\odot}$). The mass transfer begins at orbital separation of $46 R_{\odot}$. The luminosity of the donor is $21,000 L_{\odot}$. Initially, for a short period of time (6,000 yr) the mass transfer proceeds on the donor thermal timescale with the RLOF mass transfer

rate of $\dot{M}_{\text{RLOF}} = 1.2 \times 10^{-3} M_{\odot} \text{ yr}^{-1}$ (corresponding to $L_{\text{x,max}} = 5.8 \times 10^{42} \text{ erg s}^{-1}$). We allow the entire transferred material to accrete onto the BH. After mass ratio reversal, the orbit begins to expand in response to the mass transfer and the RLOF slows down. However, for the next 2,000 yr the donor RLOF rate stays above $2.2 \times 10^{-4} M_{\odot} \text{ yr}^{-1}$ ($L_{\text{x,max}} = 10^{42} \text{ erg s}^{-1}$) and the system is still classified as a potential EULX. The evolution of the mass transfer rate throughout the RLOF phase is shown in Figure 3.

The RLOF terminates when the secondary has transferred most of its H-rich envelope to the BH (with the final mass $14 M_{\odot}$). The remainder of the secondary envelope is lost in a stellar wind and the secondary becomes a naked helium star with the mass of $2.5 M_{\odot}$. At this point the binary separation is $230 R_{\odot}$. The low mass helium secondary ends its evolution in the Type Ib/c supernova explosion forming a low mass NS ($\sim 1.1 M_{\odot}$). The natal kick (if significant) is very likely to disrupt the system.

3.2. Neutron star EULX

A typical system (see NS/1 channel in Table 2 for the abbreviated evolutionary history) begins as a $10 M_{\odot}$ primary and a $5.6 M_{\odot}$ secondary on a $700 R_{\odot}$ orbit with an eccentricity $e = 0.73$. In 24 Myr the primary enters the HG. After 50,000 yr of expansion on the HG the primary overfills its Roche lobe at the radius of $85 R_{\odot}$. The orbit circularizes and becomes $190 R_{\odot}$. We assume a non-conservative mass transfer in such a case, and allow 50% of transferred material to accumulate on the main sequence secondary. At the end of this RLOF episode the primary becomes a low-mass helium star ($2.2 M_{\odot}$) and the secondary becomes a rejuvenated main sequence star ($9.5 M_{\odot}$). The separation has expanded to $640 R_{\odot}$. The low mass helium star evolves and expands after its core He burning is completed. When the radius of the primary ($200 R_{\odot}$) exceeds its Roche lobe, the second phase of a non-conservative mass transfer is initiated. At this point the separation is $720 R_{\odot}$ and the masses are $2.06 M_{\odot}$ and $9.45 M_{\odot}$ for the primary and secondary, respectively. After a short phase of a RLOF (4,000 yr) and after 28.6 Myr since the zero age main sequence (ZAMS), the primary explodes in electron capture supernova and forms a low mass NS ($1.26 M_{\odot}$). We assume zero natal kick in this case and the system survives the explosion.

After additional 20 Myr the $9.3 M_{\odot}$ secondary leaves the main sequence and evolves through the HG to become a red giant. Expansion on the red giant branch leads to a RLOF that due to a large mass ratio and a deep convective envelope of the secondary turns into a CE phase. At the onset of the CE, the separation is $600 R_{\odot}$ and the secondary radius is $330 R_{\odot}$. We assume energy balance for the CE (Webbink 1984), and obtain the post-CE separation of $50 R_{\odot}$. The secondary has lost its entire H-rich envelope and becomes a low-mass helium star ($2 M_{\odot}$). After core helium burning, the low mass secondary begins to expand and finally overfills its Roche lobe at the radius of $27 R_{\odot}$ (the corresponding binary separation is $55 R_{\odot}$). At this point the evolved helium star crosses the Helium Hertzsprung Gap and drives a high rate mass transfer ($\dot{M}_{\text{RLOF}} = 7.8 \times 10^3 M_{\odot} / \text{yr}$; $L_{\text{x,max}} = 8 \times 10^{43} \text{ erg s}^{-1}$) onto its NS companion. Since in our first approximation we have assumed a fully ef-

ficient accretion with no limit, the NS mass quickly increases to $2M_{\odot}$. The RLOF phase is very short (100 yr), and it drives an extremely high mass transfer rate allowing this system to become a potential EULX with a NS accretor (see Figure 4). Finally, the secondary is depleted of its He-rich envelope and forms a naked CO core that cools off to become a CO WD. After 51.6 Myr since the ZAMS we note the formation of a wide NS-WD binary (separation of $60 R_{\odot}$), with the gravitational merger time exceeding the Hubble time ($t_{\text{merger}} = 2.8 \times 10^{14}$ yr).

4. DISCUSSION

In this paper we presented evolutionary routes that may potentially lead to the formation of an EULX: a binary system with a compact star exhibiting X-ray luminosities in excess of 10^{42} erg s $^{-1}$. By allowing all matter transferred through the RLOF to be accreted and converted into X-rays ($\dot{M}_{\text{acc}} = \dot{M}_{\text{RLOF}}$), we are able to form a large number of potential BH and NS EULX systems. Maximum luminosities that we find in our simulations are as high as 8×10^{44} erg s $^{-1}$ (achieved for a $12 M_{\odot}$ BH accretor and a $9 M_{\odot}$ AGB companion; such high accretion lasts only for 4 yr). Particularly, the presence of the potential EULXs with NS accretors in our results seems to agree with the recent discovery of the NS ULX system M82 X-2 (Bachetti et al. 2014).

The non-limited accretion scenario leads, however, to a significant overestimate of the number of the potential EULX systems in the local Universe. We find close to ~ 100 systems with a NS, and a similar number of systems with a BH within the 100 Mpc radius. Note that these numbers should be considered to be upper limits. However to date observations have revealed only one system with $L_x > 10^{42}$ erg s $^{-1}$, HLX-1 (Farrell et al. 2011).

A problem of the maximum X-ray luminosity available from a binary system in a non-limited accretion scenario was considered also by Podsiadlowski et al. (2003). However, their study was confined to only 11 evolutionary routes, only BH binary systems, and quite limited parameter space (systems composed initially of a primary with mass in the $25 - 45 M_{\odot}$ range and a $2 - 17 M_{\odot}$ secondary mass range). Rappaport et al. (2005) extended the simulations of Podsiadlowski et al. (2003) and were able to obtain ULXs with X-ray luminosities of 3×10^{42} erg s $^{-1}$ (see their Figure 11) for a $5 M_{\odot}$ BH and $9 M_{\odot}$ donor and the case B mass transfer (HG donor). This is consistent with our typical BH EULX system. Their secondaries also fill their Roche lobe due to expansion of the envelope, and the ULX phase lasts at most a few Myr (about 10,000 yr as EULX). However, their grid of parameters is far more sparse than ours, as they simulated only 52 specific evolutionary cases in comparison to our 10^9 evolutionary routes. Both studies have their advantages.

Podsiadlowski et al. (2003) and Rappaport et al. (2005) used detailed evolutionary code to obtain their results, while we have used simplified evolutionary formulae to cover larger parameter space. With our approach we could not only confirm, but also extend the previously published results, both in terms of the accretor type (NS accretors possible) and in the range of potentially available mass transfer rates on to compact accretors in close binary systems.

Since the non-limited accretion provides only a potential maximum X-ray luminosity, we proceeded with investigating the state-of-art global accretion models of the super-Eddington accretion regime. Ohsuga (2007a) performed 2-D radiation hydrodynamic simulations of supercritical accretion disks around BHs with the αP viscosity, while Sądowski et al. (2015) performed simulations of the magnetized accretion disks in general relativity using radiation MHD code KORAL. The former simulations were fed by inflowing stream of gas circularizing near $R_{\text{cir}} = 100 R_G$, while the latter were initialized as equilibrium torii threaded by seed magnetic field. Both models agree that there is significant mass loss in the accretion flow, driven either by radiation pressure itself, or by radiation pressure and the centrifugal force. The work by Ohsuga (2007a) provides a dependence of the mass accretion rate and luminosity on the mass input rate (here \dot{M}_{RLOF}). However, this result depends strongly on the assumed location of the circularization radius, i.e., it implicitly assumes that no gas is lost outside $R \approx 100 R_G$. In real RLOF systems, the outer edge of the disk is expected to be located much further (up to about 2/3 Roche lobe radius of the accretor). The other approach (Sądowski et al. 2015) was not limited by the disk truncation inside the simulation box, but rather by the computational time, which allowed flow to reach the inflow/outflow equilibrium only to radius $R_{\text{eq}} \approx 100 R_G$. Inside this region, the gas flows out as wind down to $R_{\text{wind}} \approx 20 R_G$, and shows roughly constant mass loss rate $d\dot{M}_{\text{wind}}/dR$. The total amount of gas lost in the system will therefore depend on the location of the outer disk edge, or rather the outer edge of the wind emitting region, through Eq. 2. Because of poor understanding of the dynamics in the outer region of accretion disks, we assumed $R_{\text{wind}}/R_{\text{out}} = 0.01$.

With all of these constraints presented above we are still able to breach the 10^{42} erg s $^{-1}$ EULX limit. Although, in the case of Sądowski et al. (2015) the probability of forming a binary EULX is a few orders of magnitude smaller than for the other cases. Limitation of the mass accretion rate onto the BH in models developed in Ohsuga (2007a) and Sądowski et al. (2015) results not only in lower X-ray luminosity, but also in different orbit evolution as compared to our typical EULX case presented in Fig. 3. Both effects (lower X-ray luminosity and different orbit evolution) decrease the predicted number of EULXs in the local Universe for Ohsuga (2007a) and Sądowski et al. (2015) models.

If winds are produced effectively, matter which cannot be accreted is ejected from the system and takes away angular momentum. As a result the binary separation decreases and this prevents longer phases of high mass transfer. For the case of the Ohsuga (2007a) outflow model, the total time spent in the EULX regime is about 3,000 yr, as opposed to 10,000 yr in the non-limited accretion scenario. As a result the estimated upper limit on the number of the potential BH EULXs drops from ~ 100 to 37 EULXs in Ohsuga (2007a) model within the 100 Mpc radius. In Fig. 3 we show how the \dot{M}_{RLOF} of our typical BH EULX (non-limited accretion) translates into L_x and \dot{M}_{acc} with these constraints derived from the model of Ohsuga (2007a).

When we limit the \dot{M}_{acc} according to Eq. 2 (Sądowski

et al. 2015), we find considerably fewer BH EULXs within the 100 Mpc radius than in the case of non-limited accretion (factor of $\sim 5 \times 10^4$ fewer) and accretion limited case employing the model of Ohsuga (2007a) (factor of ~ 3 fewer). Particularly, in the case of our typical BH EULX system (Fig. 3) we find 2 orders of magnitude smaller luminosity in the beam than in the model with unlimited accretion. In Fig. 3 we show the \dot{M}_{acc} and a range of L_x computed for $\theta = 0 - 0.5$ (Eqs. 2 and 3, respectively. Sądowski et al. 2015) corresponding to the mass transfer history \dot{M}_{RLOF} of our typical BH EULX (non-limited accretion).

Both Ohsuga (2007a) and Sądowski et al. (2015) considered accretion disks around BHs. The case of a NS accretion is far more complicated. A strong magnetic fields associated with NSs may disrupt the disk far away from the accretor. Even if the magnetic field is weak, the emission will be weaker as the accretor mass is lower. On the other hand, the NS accretion efficiency (η) is higher than that of BHs as the matter and photons do not fall under the event horizon. To date, valuable simulations of such a case have not been performed. Ohsuga (2007b) performed 2D simulations for a very limited range of initial parameters. They obtained supercritical accretion rates for NS accretors and provided information that the mass accretion rate is 20-30% of that on to the BH for the same mass-input rate. Thus, we have assumed NS Eddington limited accretion case in the Ohsuga et al. models, but we have allowed super-Eddington accretion for Sądowski et al. models.

Gladstone et al. (2013) and Heida et al. (2014) presented programs to search for the companion stars of the ULX systems in the optical and infrared bands, respectively. The former group investigated close (~ 5 Mpc) ULXs and discovered 13 ± 5 optical counterparts among 33 ULXs. The masses of the companions are very inaccurate and generally only the upper limit is provided in the mass range 5.7–16.1 M_{\odot} . In a few cases the lower limit is also present in the mass range 8.3–14.7 M_{\odot} . These constraints are in agreement with our results. Heida et al. (2014) investigated 62 close ULXs and discovered 17 potential counterpart candidates. Based on the absolute magnitudes most of them (11) are Red Supergiants. According to our results the most common companions of the ULX systems able to reach the EULX regime are 6 M_{\odot} Hertzsprung gap stars with BH accretors and 1 – 2 M_{\odot} low mass Helium stars for NS accretors. However, it is possible that the Red Supergiants that we found to be in minority among the EULX companions, are more typical in the case of standard ULX systems. Detailed investigation of the properties of the entire ULX population will be presented in our forthcoming paper.

5. CONCLUSIONS

We conducted a proof-of-concept study to investigate if a binary system can form an ULX with the extreme mass transfer rate potentially able to lead to the X-ray luminosities in the $> 10^{42}$ erg s $^{-1}$ range. This is at least hundred times more than what is expected for the Eddington limited stellar mass 100 M_{\odot} BH (Belczynski et al. 2010, 2014). Observations of HLX-1 in ESO 243-49 with X-ray luminosity of 1.1×10^{42} erg s $^{-1}$ encouraged us to look into the problem.

We find several evolutionary channels that lead to phases of a very high mass transfer rate in close RLOF binaries. The mass transfer rate is so high that (if Eddington limit, or any similar limit is breached) the X-ray luminosity may reach well above 10^{42} erg s $^{-1}$. These evolutionary phases may be extremely short, but it appears that many binaries experience such phases and all observed and many to be yet discovered extreme ULXs with X-ray luminosities above 10^{42} erg s $^{-1}$ may be very easily explained by typical binary stars residing in Milky Way and nearby galaxies.

It is found that about half of this potential extreme ULX systems host not BH, but NS accretors. This contradicts the present consensus in the community, as the brightest ULX systems are commonly suspected to host IMBH primaries. Or at the minimum stellar-origin BHs.

Even in the presence of strong outflows from the accretion disk, when the accretion rate on the compact object is lower than the RLOF rate, we were able to obtain EULX sources. The mass accretion may be much weaker than in our most favorable case (no limit on X-ray luminosity) but even if the currently recognized physical constraints are imposed on the accretion rate onto compact objects the extreme luminosities ($L_x > 10^{42}$ erg s $^{-1}$) are generated in typical binary stars. It is worth to note, that nature usually finds it easy to overcome many laboratory limits that we consider the current state-of-the-art understanding of physical processes.

Our calculations show that it is possible to explain the extreme X-ray luminosities of non-nuclear point sources without invoking a presence of any so far unconfirmed entities.

We would like to thank volunteers whose participation in the universe@home test project³ made it possible to acquire the results in such a short time. This study was partially supported by the Polish NCN grant N203 404939, Polish FNP professorial subsidy "Master2013" and by Polish NCN grant SONATA BIS 2. MS was partially supported by the Polish NCN grant No. 2011/03/B/ST9/03459. KB also acknowledges NASA Grant Number NNX09AV06A and NSF Grant Number HRD 1242090 awarded to the Center for Gravitational Wave Astronomy, UTB.

REFERENCES

- Abramowicz, M., & Straub, O. 2008, NAR, 51
 Bachetti, M., Rana, V., Walton, D. J., et al. 2013, ApJ, 778, 163
 Bachetti, M., Harrison, F. A., Walton, D. J., et al. 2014, Nature, 514, 202
 Begelman, M. C., King, A. R., & Pringle, J. E. 2006, MNRAS, 370, 399
 Belczynski, K., Bulik, T., Fryer, C. L., et al. 2010, ApJ, 714, 1217
 Belczynski, K., Buonanno, A., Cantiello, M., et al. 2014, ApJ, 789, 120
 Belczynski, K., Kalogera, V., Rasio, F. A., et al. 2008a, ApJS, 174, 223

³ <http://universeathometest.info>

- Belczynski, K., Taam, R. E., Rantsiou, E., & van der Sluys, M. 2008b, *ApJ*, 682, 474
- Colbert, E. J. M., & Mushotzky, R. F. 1999, *ApJ*, 519, 89
- Crowther, P. A., Schnurr, O., Hirschi, R., et al. 2010, *MNRAS*, 408, 731
- Dominik, M., Berti, E., O’Shaughnessy, R., et al. 2014, *ArXiv e-prints*, arXiv:1405.7016
- Fabbiano, G., Gioia, I. M., & Trinchieri, G. 1989, *ApJ*, 347, 127
- Fabrika, S., Karpov, S., Abolmasov, P., & Sholukhova, O. 2006, in *IAU Symposium, Vol. 230, Populations of High Energy Sources in Galaxies*, ed. E. J. A. Meurs & G. Fabbiano, 278–281
- Farrell, S. A., Servillat, M., Wiersema, K., et al. 2011, *Astronomische Nachrichten*, 332, 392
- Fender, R., & Belloni, T. 2004, *ARA&A*, 42, 317
- Gladstone, J. C., Copperwheat, C., Heinke, C. O., et al. 2013, *ApJS*, 206, 14
- Heida, M., Jonker, P. G., Torres, M. A. P., et al. 2014, *MNRAS*, 442, 1054
- Kalogera, V., & Webbink, R. F. 1996, *ApJ*, 458, 301
- King, A. R. 2008, *MNRAS*, 385, L113
- King, A. R., Davies, M. B., Ward, M. J., Fabbiano, G., & Elvis, M. 2001, *ApJ*, 552, L109
- Kroupa, P., & Weidner, C. 2003, *ApJ*, 598, 1076
- Lasota, J.-P., King, A. R., & Dubus, G. 2015, *ApJ*, 801, L4
- Liu, J. 2011, *ApJS*, 192, 10
- Medvedev, A. S., & Poutanen, J. 2013, *MNRAS*, 431, 2690
- Miller, M. C., & Hamilton, D. P. 2002, *MNRAS*, 330, 232
- Motch, C., Pakull, M. W., Soria, R., Grisé, F., & Pietrzyński, G. 2014, *Nature*, 514, 198
- Narayan, R., Sądowski, A., Penna, R. F., & Kulkarni, A. K. 2012, *MNRAS*, 426, 3241
- Ohsuga, K. 2007a, *ApJ*, 659, 205
- . 2007b, *PASJ*, 59, 1033
- Pasham, D. R., Strohmayer, T. E., & Mushotzky, R. F. 2014, *Nature*, 513, 74
- Podsiadlowski, P., Rappaport, S., & Han, Z. 2003, *MNRAS*, 341, 385
- Poutanen, J., Lipunova, G., Fabrika, S., Butkevich, A. G., & Abolmasov, P. 2007, *MNRAS*, 377, 1187
- Rappaport, S. A., Podsiadlowski, P., & Pfahl, E. 2005, *MNRAS*, 356, 401
- Sądowski, A., Narayan, R., McKinney, J. C., & Tchekhovskoy, A. 2014, *MNRAS*, 439, 503
- Sądowski, A., Narayan, R., Tchekhovskoy, A., et al. 2015, *MNRAS*, 447, 49
- Servillat, M., Farrell, S. A., Lin, D., et al. 2011, *ApJ*, 743, 6
- Sutton, A. D., Roberts, T. P., Gladstone, J. C., & Walton, D. J. 2015, *ArXiv e-prints*, arXiv:1503.01711
- Sutton, A. D., Roberts, T. P., Walton, D. J., Gladstone, J. C., & Scott, A. E. 2012, *MNRAS*, 423, 1154
- Villante, F. L., Serenelli, A. M., Delahaye, F., & Pinsonneault, M. H. 2014, *ApJ*, 787, 13
- Walton, D. J., Roberts, T. P., Mateos, S., & Heard, V. 2011, *MNRAS*, 416, 1844
- Walton, D. J., Fuerst, F., Harrison, F., et al. 2013, *ApJ*, 779, 148
- Webbink, R. F. 1984, *ApJ*, 277, 355
- Wiersema, K., Farrell, S. A., Webb, N. A., et al. 2010, *ApJ*, 721, L102
- Yusof, N., Hirschi, R., Meynet, G., et al. 2013, *MNRAS*, 433, 1114

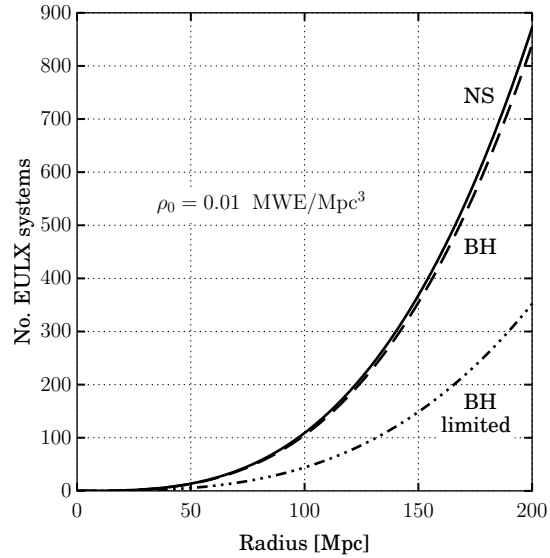


FIG. 1.— Upper limits on a number of binary extreme ULXs within the sphere of the radius R . The results are shown separately for binaries with black hole and neutron star accretors. The upper limits are obtained under assumption that a compact object can accrete at an arbitrary high rate. The lower line is for the limited accretion as obtained with formulas from Ohsuga (2007a). Using the prescription from Sądowski et al. (2015) we obtained 0.004 EULX in the sphere of 100 Mpc. Note that had we imposed the classical Eddington limit in our evolutionary model, the predicted number of extreme ULXs would be zero.

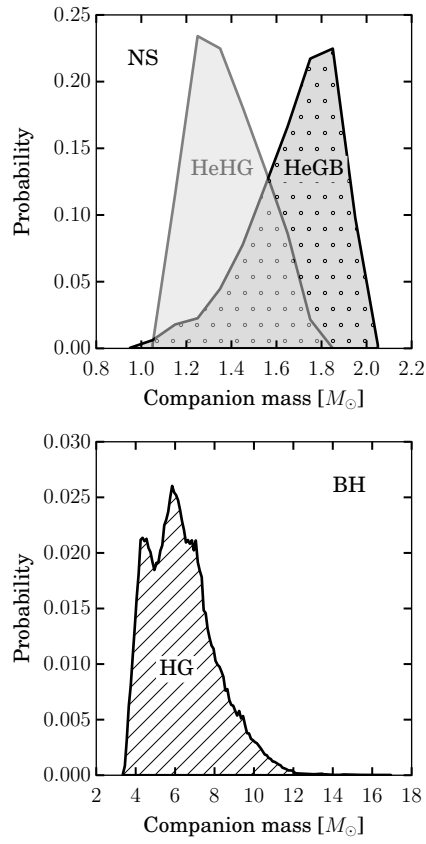


FIG. 2.— Mass distributions of the most common EULX companions in systems with a NS (top) and in systems with a BH (bottom). In the standard scenario a companion to NS evolves and during mass transfer becomes a Helium Giant Branch star starting as a Helium Hertzsprung Gap. For a BH nearly all companions are on the Hertzsprung Gap and have masses between 4 – 10 M_{\odot} .

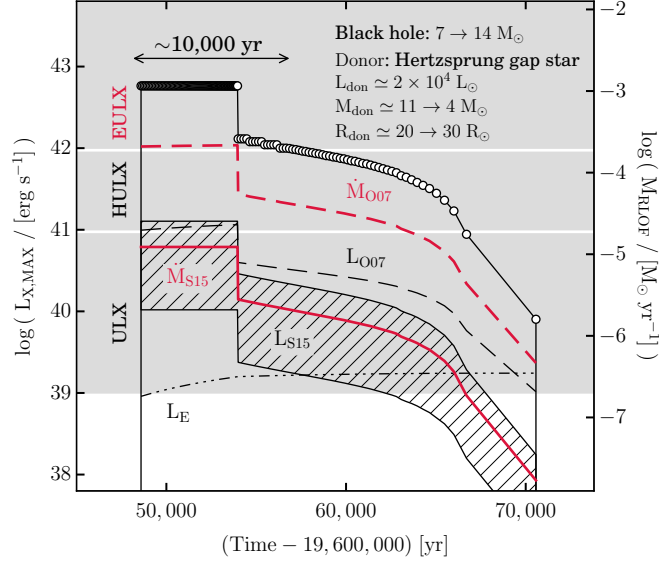


FIG. 3.— Typical evolution through Roche lobe overflow for a potential black hole extreme ULX binary. A $10 M_{\odot}$ Hertzprung gap star transfers its H-rich envelope to a $7 M_{\odot}$ black hole. The mass transfer is driven on a thermal timescale of the donor ($\sim 10,000$ yr) at the very high rate $\sim 10^{-3} M_{\odot} \text{ yr}^{-1}$. If *all* material is allowed to accrete onto a black hole the corresponding X-ray luminosity exceeds significantly $10^{42} \text{ erg s}^{-1}$. We provide in this figure limits for the luminosity and accretion as obtained by Ohsuga (2007a) (O07) and Sądowski et al. (2015) (S15). For S15 the luminosity is provided as a range as it depends on the viewing angle θ (see equation 3). The classical Eddington limit is provided as L_E . For more information see § 3.1.

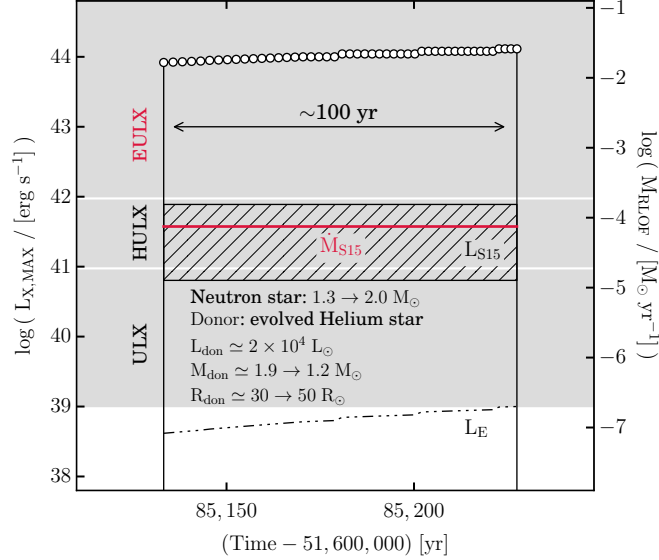


FIG. 4.— Typical evolution through Roche lobe overflow for a potential neutron star extreme ULX binary. A $1.9 M_{\odot}$ evolved helium star transfers its He-rich envelope to a neutron star. The mass transfer driven on a very short timescale lasts only ~ 100 yr until the entire envelope of the donor ($\sim 0.7 M_{\odot}$) is exhausted. The thermal timescale mass transfer rate is at the level of $\sim 10^{-2} M_{\odot} \text{ yr}^{-1}$ and the corresponding maximum X-ray luminosity exceeds $10^{42} \text{ erg s}^{-1}$. We provided also the Luminosity and mass accretion rate as obtained with formulas of Sądowski et al. (2015). However, we note here that this formulas were obtained for BH accretor. The luminosities should be smaller for the NS as the accretor mass is smaller but the effectivity of the accretion is larger. For more information see § 3.2.

TABLE 1
COMPACT ACCRETORS AND THEIR TYPICAL COMPANIONS

Accretor type ^a		Companion type ^b					
NS EULX	RG	EAGB	HeHg	HeGB	CO WD	ONe WD	
$2.6 \times 10^{-3}/\text{MWEG}$	6.35%	$6.4 \times 10^{-3}\%$	48%	44%	0.5%	0.8%	
BH EULX	MS	HG	RG	CHeB	EAGB	HeHG	HeGB
$2.5 \times 10^{-3}/\text{MWEG}$	3.4%	92.4%	1%	0.3%	0.5%	0.5%	0.3%

^a Type of the accretor and the number of EULXs in the Milky Way Equivalent galaxy

^b Percentage of EULX systems with the same accretor.

TABLE 2
TYPICAL EULX EVOLUTIONARY ROUTES

Accretor/route	% ^b	Number/MWEG ^c	Evolutionary route ^d
NS/1	50%	1.3×10^{-3}	MT1(2/3-1) MT1(8/9-1) SN1 CE2(13-3/4;13-7) MT2(13-8/9)
NS/2	40%	1.0×10^{-3}	MT1(2/3-1) SN1 CE2(13-3/4;13-7) MT2(13-8/9)
NS/3	10%	2.6×10^{-4}	Other
BH/1	97%	2.5×10^{-3}	CE1(4-1;7-1) SN1 MT2(14-1/2/3/4/5)
BH/2	3%	6.8×10^{-5}	Other

^a Percentage of the systems with the same type of the accretor.

^b Number of systems expected to be observed per Milky-Way Equivalent galaxy.

^c Symbolic designation of the evolutionary routes. MT1/MT2 is the mass from the primary/secondary, SN1 is the supernova explosion. CE1/CE2 is the common envelope started by primary/secondary. Numbers inside parenthesis specify the evolutionary phases of the stars (see Belczynski et al. (2008a) for details).